Inorganic Clusters as Single-Source Precursors for Preparation of CdSe, ZnSe, and CdSe/ZnS Nanomaterials

Scott L. Cumberland, Khalid M. Hanif, Artjay Javier, Gregory A. Khitrov, Geoffrey F. Strouse,* Stephen M. Woessner, and C. Steven Yun

Department of Chemistry and Biochemistry, University of California at Santa Barbara, Santa Barbara, California 93106

Received July 31, 2001. Revised Manuscript Received February 25, 2002

Molecular inorganic clusters, which are stable under ambient conditions, can be used as convenient single-source precursors for controlled preparation of 2−9-nm CdSe and CdSe/ZnS nanocrystals and 2−5-nm nanocrystals of ZnSe. The use of a cluster-based single-source precursor allows nanomaterial growth to be initiated at low temperature without the pyrolytic step for nucleus formation traditionally required for lyothermal growth processes. The elimination of the pyrolytic step allows greater synthetic control, slow thermodynamic growth at lower temperatures, high crystallinity, and reaction scalability (>50 g/L) while maintaining size dispersity at ∼5%.

Introduction

The observation of quantum-confinement effects in semiconductor nanomaterials has generated substantial interest for applications for device technologies utilizing the novel optical and transport properties in these structures.[1,2] The trend in nanomaterial synthesis has been the development of smaller, highly uniform, lower-dimensionality materials (quantum dots) where the quantum-confinement effects are large. In fact, the great strides in understanding the physical properties of these materials can be linked to developments in solvothermal preparative routes that allow monodisperse (metal and semiconductor) quantum dots to be readily prepared with high optical quality and a high degree of crystallinity.[3] As interest in these materials shifts from fundamental studies to the use of these materials in device applications, the focus has shifted to the development of a reliable and reproducible method for large-scale synthesis (greater than 1 g) of organically passivated materials exhibiting mono-dispersity in shape and size (<5% size dispersity).[1m]

The first reported routes to nanoparticles were the controlled precipitation of dilute colloidal solutions and the rapid termination of growth following nucleation, producing semiconductor colloids (seeds).[4−8] The growth process was described as a thermodynamic competition between the growth of larger particles and the dissolution of smaller (less stable) particles, known as Ostwald ripening. Attempts to control dispersity by growth in defined cavities resulted in the extension of these studies to growth of nanoscale materials in zeolites,[9,10] molecular sieves,[11] polymers,[12] and micelles[13] (including reverse micelles[14−16]). These colloidal methods permit large quantities of both semiconductor and metal na-

* Corresponding author: Prof. G. F. Strouse. Fax: 805.893.5326. E-mail: Strouse@chem.ucsb.edu.

(1) (a) Eychmuller, A. *J. Phys. Chem.* **2000**, *104*, 6514. (b) Brus, L. *J. Phys. Chem.* **1986**, *90*, 2555. (c) Brus, L. E. *Appl. Phys. A* **1991**, *53*, 465. (d) Nirmal, M.; Brus, L. *Acc. Chem. Res.* **1999**, *32*, 407. (e) Brus, L. E.; Trautman, J. K. *Philosoph. Trans. R. Soc. (London) A* **1995**, *353*, 313. (f) Wang, Y.; Herron, N. *J. Phys. Chem.* **1991**, *95*, 525. (g) Banyai, L.; Koch, S. W. *Semiconductor Quantum Dots*; World Scientific: Singapore, 1993. (h) Weller, H. *Angew. Chem., Int. Ed. Engl.* **1993**, *32*, 41. (i) Weller, H. *Adv. Mater.* **1993**, *5*, 88. (j) Alivisatos, A. P. *J. Phys. Chem.* **1996**, *100*, 13226. (k) Waggon, U. *Optical Properties of Semiconductor Quantum Dots*; Springer-Verlag: Berlin, 1997. (l) Gaponenko, S. V. *Optical Properties of Semiconductor Nanocrystals*; Cambridge University Press: New York, 1998. (m) Green, M.; O'Brien, P. *Chem. Commun.* **1999**, 2235. (n) Henglein, A. *Top. Curr. Chem.* **1988**, *143*, 113. (o) Henglein, A. *Chem. Rev.* **1989**, *89*, 1861.

(2) (a) Klein, D. L.; Roth, R.; Lim, A. K. L.; Alivisatos, A. P.; McEuen, P. L. *Nature* **1997**, *389*, 699. (b) Feldheim, D. L.; Keating, C. D. *Chem. Soc. Rev.* **1998**, *28*, 1. (c) Colvin, V. L.; Schlamp, M. C.; Alivisatos, A. P. *Nature* **1994**, *370*, 354. (d) Dabbousi, B. O.; Bawendi, M. G.; Onitsuka, O.; Rubner, M. F. *Appl. Phys. Lett.* **1995**, *66*, 1316. (e) Cordero, S. R.; Carson, P. J.; Estabrook, R. A.; Strouse, G. F.; Buratto, S. K. *J. Phys. Chem. B* **2000**, *104*, 12137−12142.

(3) Murray, C. B.; Norris, D. J.; Bawendi, M. G. *J. Am. Chem. Soc.* **1993**, *115*, 8706.

(4) (a) La Mer, V. K.; Dinegar, R. H. *J. Am. Chem. Soc.* **1950**, *72*, 4847. (b) Johnson, T.; La Mer, V. K. *J. Am. Chem. Soc.* **1947**, *69*, 1184.

(5) Hunter, R. J. *Foundations of Colloid Science*, 6th ed; Oxford University Press: New York, 1993; Vol. 1, pp 13−17.

(6) (a) Rossetti, R.; Nakahnara, S.; Brus, L. E. *J. Chem. Phys.* **1983**, *79*, 1986. (b) Rossetti, R.; Ellison, J. L.; Gibson, J. M.; Brus, L. *J. Chem. Phys.* **1984**, *80*, 4464.

(7) Henglein, A. *Pure Appl. Chem.* **1984**, *56*, 1215.

(8) Rossetti, R.; Hull, R.; Gibson, J. M.; Brus, L. E. *J. Chem. Phys.* **1985**, *82*, 552.

(9) (a) Wang, Y.; Herron, N. *J. Phys. Chem.* **1987**, *91*, 257. (b) McDougall, J. E.; Eckert, H.; Stucky, G. D.; Herron, N.; Wang, K.; Moller, T.; Bein, T.; Cox, D. *J. Am. Chem. Soc.* **1989**, *111*, 8006.

(10) Brigham, E. S.; Weisbecker C. S.; Rudzinski, W. E.; Mallouk, T. E. *Chem. Mater.* **1996**, *8*, 2121.

(11) Abe, T.; Tachibana, Y.; Uematsu, T.; Iwamoto, M. *J. Chem. Soc., Chem. Commun.* **1995**, 1617.

(12) (a) Wang, Y.; Suna, A.; Mahler, W.; Kasowski, R. *J. Chem. Phys.* **1987**, *87*, 7315. (b) Fotjik, A.; Weller, H.; Koch, U.; Henglein, A. *Ber. Bunsen-Ges. Phys. Chem.* **1984**, *88*, 969. (c) Haggata, S. W.; Cole-Hamilton, D. J.; Fryer, J. R. *J. Mater. Chem.* **1996**, *7*, 1969.

(13) Watzke, H. J.; Fendler, J. H. *J. Phys. Chem.* **1987**, *91*, 854.

(14) (a) Kortan, A. R.; Hull, R.; Opila, R. L.; Bawendi, M. G.; Stiegerwald, M. L.; Carroll, P. J.; Brus, L. E. *J. Am. Chem. Soc.* **1990**, *112*, 1327. (b) Steigerwald, M. L.; Alivisatos, A. P.; Gibson, J. M.; Harris, T. D.; Kortan, R.; Muller, A. J.; Thayer, A. M.; Duncan, T. M.; Douglass, D. C.; Brus, L. E. *J. Am. Chem. Soc.* **1988**, *110*, 3046.

(15) Meyer, M.; Walberg, C.; Kurihara, K.; Fendler, J. H. *J. Chem. Soc., Chem. Commun.* **1984**, 90.

(16) Lianos, P.; Thomas, J. K. *Chem. Phys. Lett.* **1986**, *125*, 299. Ingert, D.; Pileni, M. P. *Adv. Func. Mater.* **2001**, *11*, 136 and references therein.

10.1021/cm010709k CCC: $22.00
Published on Web 03/27/2002

nomaterials to be produced from readily available precursors; however, most of these methods tend to yield nanoparticles with large size dispersities on the order of 10%. Continued improvements in the synthesis of materials using arrested precipitation and inverse micelle techniques have led to high-quality monodisperse metal and semiconductor nanocrystals under appropriate conditions.[17]

The reproducibility of size dispersity and crystallinity was largely surmounted by the development of lyothermal techniques, i.e., the thermal degradation of organometallic precursors.[18−21] Lyothermal methodology allows a large series of organically passivated materials exhibiting near monodispersity (<5%) to be generated via pyrolytic degradation of an air-sensitive, thermally unstable organometallic precursor.[3,22−35] Extrapolation of standard lyothermal methods to the use of air-stable, nonorganometallic precursors based on CdO and Cd(OAc)$_2$ has been shown to produce high-quality CdSe materials by a similar pyrolytic nucleation event. [26a,26c,36]

The development of lyothermal techniques demonstrated that high-temperature reactions are critical to crystallinity, allowing lattice glide plane defects to anneal out.[22,23] The control of size dispersity in both semcionductor and metal nanoparticles prepared by lyothermal strategies is believed to be controlled by the separation of core nucleation from material growth via a competition of thermodynamic rates and kinetic processes for the reaction mixture.[22,23] Analysis of the reaction mechanism indicates that the selection of passivating solvent, reaction precursors, and reaction conditions are all critical to control of the material dispersities and material topoloigies.[3,22,23] Lyothermal routes are highly dependent on the nature of the materials being prepared, with CdSe exhibiting the greatest control and InP far less control over growth.[24] In the case of the Cd chalcogenide II−VI materials, CdSe is more easily controlled lyothermally, in comparison to CdS and CdTe. Much of the difference in reaction behavior arises from the nature of the metal or binary semiconductor constituents due to differences in the chemical reactivity. In particular, differences in reactivity, material quality, particle size, and particle dispersity can be roughly correlated to the differences in Bohr radius, oxidative stability, strength of electron−electron interactions, electron−phonon interactions, and ionicity of the respective metal−chalcogenide lattices.[37]

A new direction for nanomaterial preparation being pursued is the use of single-source precursors that are stable under ambient conditions and have the metal−chalcogen bond already templated in the molecular precursor. O'Brien and co-workers have demonstrated the use of pyrolyzable single-source molecular precursors based on metal dithio- and diselenocarbamate complexes for the preparation of CdS, ZnS, ZnSe, and CdSe.[38−40] The use of single-source precursors with preformed metal−chalcogenide bonds provides a convenient reactive intermediate for growth under lyothermal conditions, allowing for the preparation of large quantities of materials from relatively innocuous reagents.

Inorganic clusters are a class of materials that might potentially be ideal for application as single-source precursors. Inorganic clusters, as a class of materials, exist as discrete units with structures related to a fragment of a bulk lattice.[41−56] Previous NMR and mass spectroscopy studies on exchange dynamics in metal−chalcogenide clusters consisting of $[M_{10}Se_4(SPh)_{16}]^{4-}$ (where M = Cd, Zn and SPh is thiophenolate) suggest

(17) (a) Alvarez, M. M.; Khoury, J. T.; Schaaff, T. G.; Shafigullin, M.; Vezmar, I.; Whetten, R. L. *Chem. Phys. Letts* **1997**, *266*, 91−98. (b) Brust, M.; Kiely, C. J.; Bethell, D.; Schiffrin, D. J. *J. Am. Chem. Soc.* **1998**, *120*, 12367−12368. (c) Wilcoxon, J. P.; Martin, J. E.; Provencio, P. *Langmuir* **2000**, *16*, 9912−9920. (d) Ridley, B. A.; Nivi, B.; Jacobson, J. M. *Science* **1999**, *286*, 746.

(18) Brennan, J. G.; Siegrist, T.; Carroll, P. J.; Stuczynski, S. M.; Reynders, P.; Brus, L. E.; Steigerwald, M. L. *Chem. Mater.* **1990**, *2*, 403.

(19) Brennan, J. G.; Siegrist, T.; Carroll, P. J.; Stuczynski, S. M.; Brus, L. E.; Steigerwald, M. L. *J. Am. Chem. Soc.* **1989**, *111*, 4141.

(20) Steigerwald, M. L.; Struczynski, S. M.; Kwon, Y. U.; Vennos, D. A.; Brennan, J. G. *Inorg. Chim. Acta* **1993**, *212*, 219.

(21) Steigerwald, M. L. *Polyhedron* **1994**, *13*, 1245.

(22) Katari, J. E. B.; Colvin, V. L.; Alivisatos, A. P. *J. Phys. Chem.* **1994**, *98*, 4109.

(23) Peng, X.; Wickham, J.; Alivisatos, A. P. *J. Am. Chem. Soc.* **1998**, *120*, 5343.

(24) Guzelian, A. A.; Katari, J. E. B.; Kadavanich, A. V.; Banin, U.; Hamad, K.; Juban, E.; Alivisatos, A. P.; Wolters, R. H.; Arnold, C. C.; Heath, J. R. *J. Phys. Chem.* **1996**, *100*, 7212−7219.

(25) Manna, L.; Scher, E. C.; Alivisatos, A. P. *J. Am. Chem. Soc.* **2000**, *122*, 12700.

(26) (a) Peng, Z. A.; Peng, X. *J. Am. Chem. Soc.* **2001**, *123*, 183. (b) Peng, Z. A.; Peng, X. *J. Am. Chem. Soc.* **2001**, *123*, 1389. (c) Qu, L.; Peng, Z. A.; Peng, X. *Nano Lett.* **2001**, *1*, 333.

(27) Peng, X.; Manna, L.; Yang, W.; Wickham, J.; Scher, E.; Kadavanich, A.; Alivisatos, A. P. *Nature* **2000**, *404*, 59.

(28) Guzelian, A. A.; Banin, U.; Kadavanich, A. V.; Peng, X.; Alivisatos, A. P. *Appl. Phys. Lett.* **1996**, *69*, 1432.

(29) Olshavsky, M. A.; Goldstein, A. N.; Alivisatos, A. P. *J. Am. Chem. Soc.* **1990**, *112*, 9438.

(30) Nozik, A. J.; Micic O. I. *MRS Bull.* **1998**, *23* (2), 24 and references therein.

(31) (a) Micic, O. I.; Sprague, J. R.; Curtis, C. J.; Jones, K. M.; Machol, J. L.; Nozik, A. J.; Giessen, H.; Fluegel, B.; Mohs, G.; Peyghambarian, N. *J. Phys. Chem.* **1995**, *99*, 7754. (b) Micic, O. I.; Curtis, C. J.; Jones, K. M.; Sprague, J. R.; Nozik, A. J. *J. Phys. Chem.* **1994**, *98*, 4966.

(32) (a) Micic, O. I.; Nozik, A. J. *J. Lumin.* **1996**, *70*, 95. (b) Micic, O. I.; Sprague, J. R.; Lu, Z. H.; Nozik, A. J. *Appl. Phys. Lett.* **1996**, *68*, 3150.

(33) (a) Hines, M. A.; Gyot-Sionnest, P. *J. Phys. Chem.* **1998**, *102*, 3655. (b) Norris, D. J.; Yao, N.; Charnock, F. T.; Kennedy, T. A. *Nano Lett.* **2001**, *1*, 3.

(34) Douglas, T.; Theopold, K. H. *Inorg. Chem.* **1991**, *30*, 594.

(35) Kher, S. S.; Wells, R. L. *Nanostruct. Mater.* **1996**, *7*, 591.

(36) Yang, C.; Awschalom, D. D.; Stucky, G. D. *Chem. Mater.* **2001**, *13*, 594.

(37) Abrikosov, N. Kh.; Bankina, V. F.; Poretskaya, L. V.; Shemilova, L. E.; Skudnova, E. V.; translated by Tybulewicz, A. *Semiconducting II−VI, IV−VI, and V−VI Compounds*; Plenum Press: New York, 1969.

(38) (a) Trindade, T.; O'Brien, P. *Adv. Mater.* **1996**, *8*, 161. (b) Trindade, T.; O'Brien, P.; Zhang, X. *Chem. Mater.* **1997**, *9*, 523.

(39) Ludolph, B.; Malik, M. A.; O'Brien, P.; Revaprasdu, N. *Chem. Commun.* **1998**, 1849.

(40) Malik M. A.; Revaprasadu, N.; O'Brien, P. *Chem. Mater.* **2001**, *13*, 913.

(41) Dance, I.; Fisher, K. *Prog. Inorg. Chem.* **1994**, *41*, 637 and references therein.

(42) Dance, I. G.; Choy, A.; Scudder, M. L. *J. Am. Chem. Soc.* **1984**, *106*, 6285.

(43) Zhu, N.; Fenske, D. *J. Chem. Soc., Dalton Trans.* **1999**, 1067.

(44) Zhu, N.; Fenske, D. *J. Cluster Sci.* **2000**, *11*, 135.

(45) Muller, A.; Fenske, D.; Kogerler, P. *Curr. Opin. Solid State Mater. Sci.* **1999**, *4*, 141.

(46) (a) Schmid, G.; Chi, L. F. *Adv. Mater.* **1998**, *10*, 515. (b) Schmid, G. J. *Chem. Soc., Dalton Trans.* **1998**, 1077.

(47) Brown, K. R.; Natan, M. J. *Langmuir* **1998**, *14*, 726.

(48) Gaumet, J. J.; Strouse, G. F. *J. Am. Soc. Mass Spectrom.* **2000**, *11*, 338.

(49) *Metallothionein: Synthesis, Structure, and Properties of Metallothioneins, Phytochelatins, and Metal−Thiolate Complexes*;Stillman, M. J. M., Shaw, C. F., III, Suzuki, K. T., Eds.; VCH Publishers: New York, 1992.

(50) Hagen, K. S.; Holm, R. H. *Inorg. Chem.* **1983**, *22*, 3171. Christou, G.; Hagen, K. S.; Bashkin, J. K.; Holm, R. H. *Inorg. Chem.* **1985**, *24*, 1010. Watson, A. D.; Rao, C. P.; Dorfman, J. R.; Holm, R. H. *Inorg. Chem.* **1985**, *24*, 2820.

that rapid ligand and metal exchange at room temperature occurs in solution, coupled with a propensity to rearrange to form larger molecular clusters with the loss of $Cd(SPh)_3^-$. The rearrangement to form more thermodynamically stable species proceeds through a nonstoichiometric reaction mechanism with the formation of phenyl disulfide and $Cd(SPh)_3^-$ species.[51b,51c] Because of the inherent thermodynamic instability of the clusters, several researchers have used $[M_{10}Se_4(SPh)_{16}]^{4-}$ clusters as inorganic precursors for the growth of bulk semiconductors via direct thermal decomposition of the solid powders, as well as solvothermal decomposition in pyridine.[51d]

The propensity for formation of thermodynamically stable clusters of larger nuclearity in solvents and bulk structures in solid-state reactions suggests that these inorganic molecular clusters, although nonstoichiometric with respect to the ratio of Cd and Se in the final nanomaterials, might allow controlled growth of II−VI nanomaterials if the kinetic and thermodynamic reactions are controlled by the choice of the reaction conditions.[51,53,57] In this process, the cluster would act as a preformed nucleus capable of structural rearrangement without dissolution, thus allowing for the separation of the nucleation and growth steps using a single-source precursor without a requisite pyrolytic event to initiate nucleation.

In this paper, we present the results for a series of materials prepared by a single-source precursor methodology based on the introduction of an inorganic metal−chalcogenide cluster into an alkylamine solvent. Owing to the rapid ligand and metal exchange for these clusters, nucleation occurs instantly at low temperatures, followed by growth of nanomaterials under thermal control. This allows for the preparation of large-scale reactions of organically passivated, spherical nanomaterials (>50 g/L) of CdSe and ZnSe (<5% rms size-selectively precipitated, ∼5% thermally annealed or 6−12% out-of-batch). The CdSe can be recapped with an inorganic passivant layer (ZnS) following traditional lyothermal techniques to yield CdSe/ZnS core/shell structures. A major advantage of this new methodology is the attainment of greater synthetic control.

Experimental Section

Materials. $(X)_4[M_{10}Se_4(SPh)_{16}]$ [X = Li^+ or $(CH_3)_3NH^+$, M = Cd or Zn, and SPh is phenyl thiolate] were prepared by literature methods[42] with the exception of using a Li^+ cation instead of a tetramethylammonium cation for isolation of $[Cd_{10}Se_4(SPh)_{16}]$.[4−58] Hexadecylamine (HDA, 90%) and bis-(trimethylsilyl sulfide) were purchased from Acros Chemical and used without further purification. Dimethyl zinc (2 M solution in toluene) and trioctylphosphine (TOP, 90%) were purchased from Aldrich Chemical and used without further purification. Further purification of the precursors did not influence the reaction yields or material quality.[59]

Measurement. Ultraviolet and visible absorption spectra in chloroform or toluene were recorded using a fiber optic Ocean Optics S2000 CCD spectrophotometer. Instrument-response-corrected photoluminescence (PL) spectra were measured on a SPEX-flurolog equipped with a 400-W xenon lamp and a cooled Hamamatsu R928 photomultiplier tube (PMT). PL measurements were conducted on dilute N_2-sparged solutions with an absorption at the wavelength of excitation below 0.1 absorbance and under front face conditions to minimize self-absorption from the quantum dot solution. PL response correction files were generated with a NIST traceable 200 W quartz−halogen tungsten filament lamp (model 220M) and steady power supply using hardware and software supplied by SPEX. Correction files are routinely generated yearly for the instrumentation.

Photoluminescence quantum yield values (ϕ_{em}) were measured relative to Rhodamine 590 in methanol for CdSe and anthracene in toluene for ZnSe systems and were calculated using eq 1.[60]

$$\phi_{em} = \phi'_{em}(I/I')(A'/A)(n/n')^2 \quad (1)$$

In eq 1, I (sample) and I' (standard) are the integrated emission peak areas, A (sample) and A' (standard) are the absorbances at the excitation wavelength, and n (sample) and n' (standard) are the refractive indices of the solvents.

Transmission electron microscopy (TEM) was performed on a JEOL 2000 microscope operating at either 100 or 200 kV in the bright-field mode. The TEM magnification was calibrated by measuring the lattice fringe spacing on Au nanocrystals. TEM grids were 400-mesh Cu, coated with a 5-nm layer of holey carbon and purchased from SPI. TEM samples were prepared using standard techniques. Size and size distributions were obtained by manual measurement of nanocrystal images obtained by digitizing the micrograph negatives.

The powder X-ray diffraction (pXRD) patterns of the nanocrystals were obtained on a Scintag ×2 diffractometer using Cu Kα radiation, excited at 45 kV and 35 mA. The X-rays were collimated at the source with 2-mm divergence and 4-mm scatter slits. The detector had 0.5-mm scatter and 0.2-mm receiving slits.

Preparation of Amine-Capped CdSe Nanoparticles. Approximately 55 g of HDA was degassed under vacuum at 120 °C. To the stirred solution of HDA under N_2 was added 1.0 g (0.28 mmol) of $(Li)_4[Cd_{10}Se_4(SPh)_{16}]$ using standard airless techniques, and the solution temperature was raised to 220−240 °C (1 °C/min). Growth rates depend on the initial reactant concentration and can be followed by absorption spectroscopy. At the desired crystal size, the reaction mixture was cooled by 20 °C and left overnight to narrow the size distribution by annealing the nanocrystals. The CdSe can be isolated by selective precipitation by addition of 100 mL of

(51) (a) Wang, Y.; Herron, N. *J. Phys. Chem.* **1991**, *95*, 525. (b) Herron, N.; Suna, A.; Wang, Y. *J. Chem. Soc., Dalton Trans.* **1992**, 2329. (c) Wang, Y.; Harmer, M.; Herron, N. *Israel J. Chem.* **1993**, *33*, 31−39. (d) Herron, N.; Calabrese, J. C.; Farneth, W. E.; Wang, Y. *Science* **1993**, *259*, 1426.

(52) (a) Gaumet, J. J.; Raola, O. E.; Woessner, S. M.; Strouse, G. F., manuscript in progress. (b) Raola, O. E.; Woessner, S. M.; Strouse, G. F., manuscript in progress.

(53) Hagen, K. S.; Stephan, D. W.; Holm, R. H. *Inorg. Chem.* **1982**, *21*, 3928−3936.

(54) Hernandez-Molina, R.; Sykes, A. G. *J. Chem. Soc., Dalton Trans.* **1999**, 3137.

(55) Stiefel, E. I.; Halbert, T. R.; Coyle, C. L.; Wei, L.; Pan, W. H.; Ho, T. C.; Chianelli, R. R.; Daage, M. *Polyhedron* **1989**, *8*, 1625.

(56) Diemann, E.; Muller, A.; Aymonino, P. J. *Z. Anorg. Allg. Chem.* **1981**, *479*, 191.

(57) Løver, T.; Bowmaker, G.; Seakins, J. M.; Cooney, R. P.; Henderson, W. *J. Mater. Chem.* **1997**, *7*, 647.

(58) Crystalline $[Cd_{10}Se_4(SPh)_{16}]^{4-}$ can be prepared in a two-step synthetic reaction to form an air-stable, crystalline inorganic cluster. Briefly, the reaction is carried out through the formation of $[Cd_4(SPh)_{12}]^{2-}$ by the direct addition of a stoichiometric amount of $Cd(NO_3)_2$ to a methanol solution containing a 1:1 mole ratio of triethylamine and thiophenol under ambient conditions. Triethylamine is added to deprotonoate the thiophenol. Addition of either $LiNO_3$ or TMACl (tetramethylammonium chloride) allows for the isolation of a crystalline product. Conversion of $[Cd_4(SPh)_{12}]^{2-}$ to $[Cd_{10}Se_4(SPh)_{16}]^{4-}$ is accomplished by treatment of a room-temperature acetonitrile solution of $[Cd_4(SPh)_{12}]^{2-}$ with Se under N_2. Single crystals can be generated by recrystallization from hot acetonitrile.

(59) Dimethylzinc is pyrophoric in the presence of O_2 because of the highly exothermic formation of ZnO. TOP is oxygen-sensitive with a propensity to form the phosphine oxide and should therefore be handled under airless conditions.

(60) Demas, J. N.; Crosby, G. A. *J. Phys. Chem.* **1971**, *75*, 991.

anhydrous MeOH and centrifugation. Excess HDA was removed by subsequent resuspension in MeOH and isolation by centrifugation.

Preparation of Amine-Capped ZnSe Nanoparticles. Approximately 55 g of HDA was degassed at 120 °C for 2 h. To the stirred solution of HDA under N_2 was added 600 mg (0.20 mmol) of $(TMA)_4[Zn_{10}Se_4(SPh)_{16}]$, and the solution temperature was raised to 220−280 °C (1 °C/min). Analogous to the above reaction, the nanomaterial growth can be monitored by absorption spectroscopy and isolated by cooling the reaction to 80 °C, adding 100 mL of anhydrous methanol, and centrifuging the precipitated ZnSe nanomaterials.

Preparation of CdSe/ZnS Core/Shell Structures. The core/shell structures were prepared by a modification of the procedure developed by Hines and co-workers.[61] At the desired nanomaterial size, a 4-fold excess of a TOP solution containing equimolar dimethylzinc and bis(trimethylsilyl) sulfide was injected into the reaction mixture at 250 °C. The product was collected as described above. The amounts of dimethylzinc and bis(trimethylsilyl) sulfide were determined from the estimate of the core diameter based on absorption spectropscopy and the requisite concentration of precursor required to obtain the desired shell thickness.

Size-Selective Precipitation. Depending on the temperature ramp rate, nanomaterials can be isolated from the batch without size selection with a dispersity of 6−8% based on correlations of the results of TEM, absorption, and pXRD line widths in comparison to reported literature data.[3] For unannealed batches, 5% dispersity is achieved by narrowing the distribution by size-selective precipitation from toluene. This procedure results in center enrichment, with the isolation of ∼50% of the batch with ∼ 5% rms size distribution based on TEM analysis of the samples. Thermal annealing of the reaction mixture for 24 h allows the nanomaterials to be isolated with 5% dispersity without size-selective precipitation.

Results

Selected absorption and emission spectra of CdSe and ZnSe nanocrystals grown from $[M_{10}Se_4(SPh)_{16}]^{4-}$ (M = Cd or Zn, SPh is thiophenol) are shown in Figures 1 and 2, respectively. The two growth progressions show well-defined excitonic structure and size quantization. The sizes of the CdSe nanoparticles were estimated using absorption spectroscopy[21] and verified by TEM analysis. Representative TEM analyses of CdSe, ZnSe, and CdSe/ZnS core/shell nanocrystals exhibiting lattice fringes are illustrated in Figure 3. The absorption data for size selection of a typical reaction batch of 5.6-nm CdSe (Figure 4a represents the absorption for the initial 12% size dispersity) is shown in Figure 4. TEM size-distribution analysis of the size-selected batch (Figure 4b) shows ∼5% size dispersity can be achieved, as observed previously in TOP/TOPO-grown materials. Table 1 lists the exciton absorption maxima, exciton fwhm, and TEM distribution analysis for several sizes of CdSe and ZnSe nanoparticles. The observed quantum yields for the CdSe and CdSe/ZnSe samples are comparable to the reported quantum yields for lyothermally grown materials [3,22] Quantum yields for emission on the core/shell materials indicate an enhancement of the emission in the 3.7- and 4.5-nm CdSe/ZnS core/shell (QY = 20%) samples by approximately a factor of 2 relative to 3.7-nm (QY = 6%) and 4.5-nm (QY = 10%) HDA-passivated CdSe, consistent with earlier literature findings for inorganically vs organically passivated materials. [61−68]

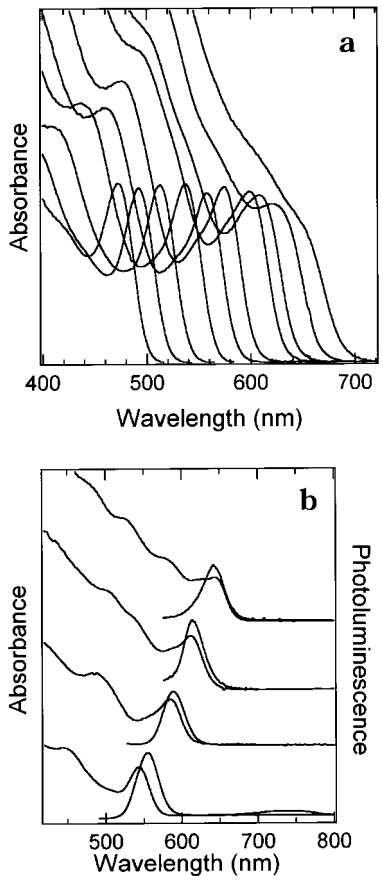

Figure 1. Normalized absorbance spectra in toluene at 298 ± 2 K of (a) batch 2.5−9.0-nm CdSe/HDA nanocrystals prepared by the single-source precursor route and (b) size-selected 3.7-, 4.5-, 6.0-, and 8.0-nm CdSe/HDA nanocrystals prepared by the single-source precursor route. Excitation was carried out at 488.0 nm and 1 mW of power.

Reaction Mechanism. The evolution of CdSe nanomaterials as a function of temperature is plotted in Figure 5. The formation of larger nanomaterials is reproducibly achieved above 220° C. ZnSe follows a similar trend in size versus temperature; however, the onset of growth occurs at higher temperature. Consistent with a thermodynamically driven reaction, the batch size distribution broadens as the temperature increases. The nanomaterial reactions can be scaled between 1 and 50 g/L; however, it should be noted that 9.0-nm CdSe is achieved only in lower concentration reactions because of the higher temperatures required for large-concentration reaction batches. In Figure 5b, the dependence of concentration on the temperature for

(61) Hines, M. A.; Gyot-Sionnest, P. *J. Phys. Chem.* **1996**, *100*, 468−471.

(62) (a) Danek, M.; Jensen, K. F.; Murray, C. B.; Bawendi, M. G. *Chem. Mater.* **1996**, *8*, 173−180. (b) Dabbousi, B. O.; Rodrigues-Viejo, J.; Miculek, F. V.; Heine, J. R.; Mattousi, H.; Ober, R.; Jensen, K. F.; Bawendi, M. G. *J. Phys. Chem. B* **1997**, *101*, 9463.

(63) Hoener, C. F.; Allan, K. A.; Bard, A. J.; Campion, A.; Fox, M. A.; Mallouk, T. E.; Webber, S. E.; White, J. M. *J. Phys. Chem.* **1992**, *96*, 3812.

(64) Kortan, A. R.; Hull, R.; Opila, R. L.; Bawendi, M. G.; Stiegerwald, M. L.; Caroll, P. J.; Brus, L. E. *J. Am. Chem. Soc.* **1990**, *112*, 1327.

(65) Tian, Y.; Newton, T.; Kotov, N. A.; Guldi, D. M.; Fendler, J. H. *J. Phys. Chem.* **1996**, *100*, 8927.

(66) Peng, X.; Schlamp, M. C.; Kadavanich, A. V.; Alivisatos, A. P. *J. Am. Chem. Soc.* **1997**, *119*, 7019.

(67) Revaprasadu, N.; Malik, M. A.; O'Brien, P.; Wakefield, G. *Chem. Commun.* **1999**, 1573−1574.

(68) Talapin, D. M.; Rogach, A. L.; Kornowski, A.; Haase, M.; Weller, H. *Nano Lett.* **2001**, *1*, 207.

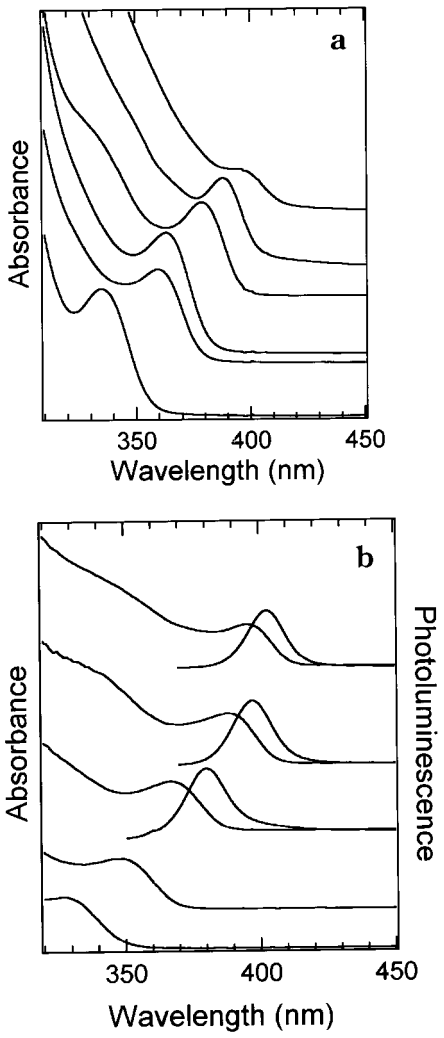

Figure 2. (a) Normalized absorbance spectra in toluene at 298 ± 2 K of batch <3.0−5.0-nm ZnSe/HDA nanocrystals and (b) 3.0- (lower two), 3.0-, 4.7-, and 5.0-nm ZnSe/HDA nanocrystals prepared by the single-source precursor route. Excitation was carried out at 325.0 nm and 1 mW of power.

nanomaterial growth is indicated for reactions on the 6-and 17-g/L scales.

Nanomaterials prepared from inorganic clusters exhibit size-dispersity annealing over a 24-h period by lowering reaction temperatures by 10 °C (Figure 6). No observable changes in size or absorption line width occur for the nanomaterials under room-temperature annealing conditions[69] (See Supplemental Figure 4). Although the nanomaterials can be annealed for periods in excess of 48 h, typical annealing times depend on the concentration of the reaction, and for 6 g/L, typical annealing times are ∼12−24 h. A reaction mechanism for formation of nanomaterials based on the earlier studies of ring opening and reconstruction of metal−chalcogenide clusters is proposed in Figure 7.

X-ray Diffraction. Powder X-ray diffraction data are provided in Supporting Information. Both CdSe (hexagonal) and ZnSe (cubic zinc blende) exhibit pXRD diffraction patterns consistent with spherical nanoparticles.[3,33a] In Supplemental Figures 1 and 2, the observed diffraction features can be assigned to lattice reflections for CdSe and ZnSe. In Supplemental Figure 3, the observed diffraction features correspond to contributions from the CdSe and ZnS overlayers. The diffraction feature at 20.62 in 2θ (0.43 nm) corresponds to the hexyldecylamine spacing on the surface of the nanocrystal.

(69) For room-temperature annealing, a hexadecylamine dispersion of CdSe was diluted by a factor of 3 with dry octylamine. Dilution in octylamine allows the reaction to be maintained at room temperature without solidification of the HDA. Room-temperature annealing was carried out for 400 h under a N_2 atmosphere with no observable change in the absorbance.

Discussion

Nanomaterial Growth. Several lyothermal techniques, and simple salt-based growth techniques in coordinating solvents have been shown to produce high-quality CdSe, CdS, CdTe, and ZnSe nanomaterials.[3,22,26,33] These methods are generalizable but are often limited to smaller-scale reactions because of the nature of the solvents, precursors, and reaction rates. Lyothermal methods typically require a pyrolytic step in excess of 300 °C, followed by sustained growth at temperatures in excess of 200 °C. Synthetic preparations at room temperature in pyridine have produced CdSe materials of high quality, although the extrapolation to other II−VI materials has not been demonstrated and the reported sizes are below 5 nm. Application of a molecular-cluster-based single-source precursor for nanomaterial growth offers an alternative synthetic methodology for material preparation that appears to be readily generalized to both Cd and Zn chalcogenide systems and that exhibits neither size restrictions on nanoparticle growth nor reaction-scale restrictions due to associated dangers of pyrolytic starting materials or hazardous growth solvents. Furthermore, the lowered growth temperatures allow reasonably priced solvents to be employed, as long as the boiling points exceed 190 °C.

The development of synthetic methodologies that allow generalizable, large-scale reactions for the production of nanomaterials is important for the application of these materials in device technologies. The application of molecular-cluster-based single-source precursors is an ideal approach for use as single-source precursors as they can be prepared under ambient conditions and purified by recrystallization techniques. This leads to an inorganic single-source precursor that exhibits a long-term shelf life under ambient conditions. Introduction of the precursor to a growth solvent at lower temperature (below 100 °C) allows for the controlled growth of the desired II−VI (CdSe or ZnSe) nanomaterial through thermodynamic control. This results in a highly scalable and versatile synthetic methodology, allowing for the growth of well-formed CdSe and ZnSe nanomaterials (Figures 1−3). CdSe, ZnSe, and CdSe/ZnS nanomaterials can be grown from inorganic clusters in alkylamine solvents to produce materials that exhibit very narrow size dispersities (Figures 1−4) based on fwhm analysis of the exciton absorbance and emission band and TEM analysis of the final product (Figure 3). The out-of-batch samples exhibit size dispersities on the order of 10−12% (Figure 4a, i), with significant improvement following selective precipitation of the materials from the reaction mixture (Figure 4a, iv). In Figures 1 and 2, the normalized absorbance and photoluminescence of size-selectively precipitated CdSe and

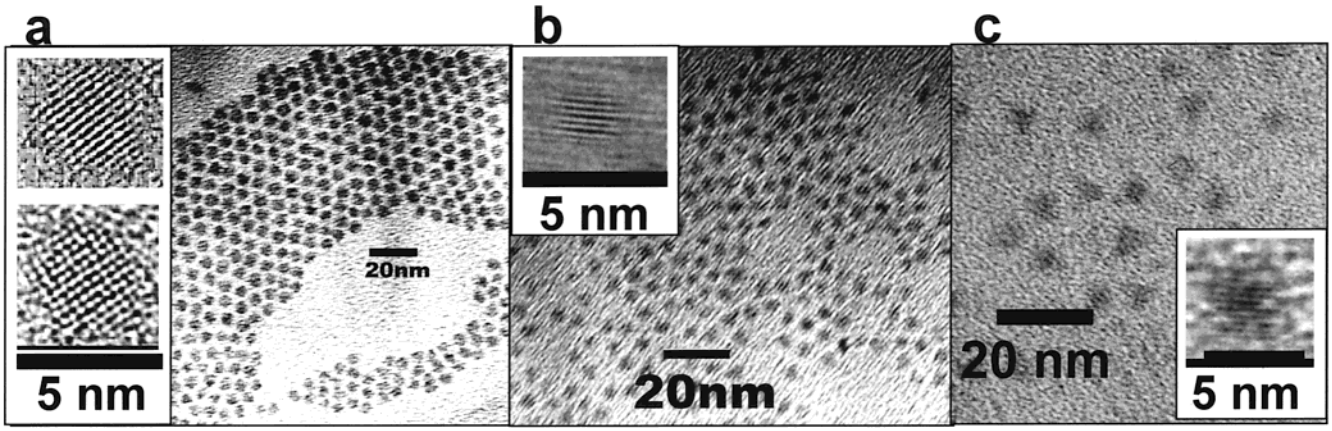

Figure 3. TEM images of (a) 4.5-nm CdSe, (b) 2.8-nm ZnSe, and (c) CdSe/ZnS core/shell nanocrystals with 3.7-nm cores and a final size of 5.4 nm deposited from toluene on a holey-carbon-coated Cu grid. Higher-magnification images of single dots are shown in the inset.

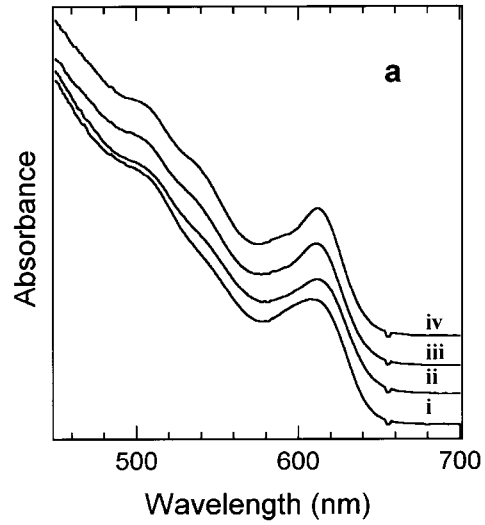

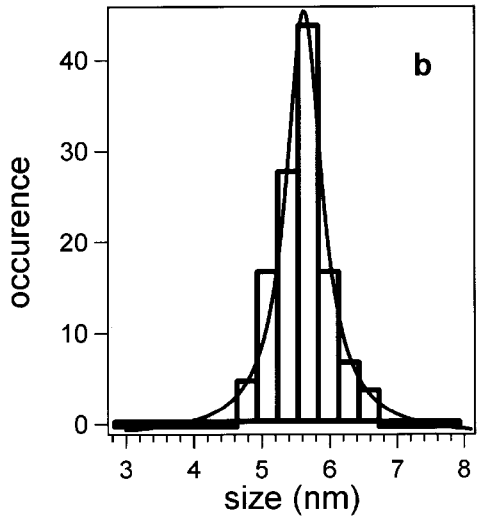

Figure 4. (a) Absorption spectrum in toluene at 298 K showing selective precipitation of 6.0-nm CdSe/HDA with dispersity ranging from (i) 12% for out-of-batch sample to (iv) 5% for a size-selected sample. (b) Size distribution of the final size-selected sample was 6.0 ± 0.30 nm and was obtained by fitting a Lorenzian function to the data (shown).

ZnSe nanocrystals exhibit a series of exciton bands, consistent with <5% distribution in the nanomaterial size. Consistent with literature reports, the second, third, fourth, and fifth excitons are more clearly resolved in the larger nanomaterials.[3] In Figure 2, the broader absorptions for ZnSe arise from poorer size distributions, as well as complications arising from the inherent oxygen instability of ZnSe nanomaterials.

Table 1. Statistics for II−VI Nanomaterials Prepared from Single-Source Precursors

size (nm)	size dispersity (%)	λ_{abs} (nm)	fwhm (nm)
	CdSe		
2.5[b]	5[c]	472	33
3.7	~5[a]	543	30
4.5[b]	5[c]	574	32
5.5	5	601	30
6.0	5	612	36
8.0	5	644	34
9.0[b]	5[c]	655	33
	ZnSe		
<2.8	~10[c]	328	26
<2.8	~10[c]	348	26
2.8	~7[a,c]	363	22
4.5[b]	~7[c]	388	22
4.8	7	393	18

[a] TEM image limits the accuracy of the dispersity analysis. [b] Estimated from λ_{abs}. [c] Estimated from fwhm.

TEM data on spherical samples isolated from the reaction mixture by selective precipitation for 4.5-nm CdSe, 5.4-nm CdSe/ZnS core/shell, and 2.8-nm ZnSe nanomaterials exhibit distinct lattice fringes and well developed patterns that are consistent with the formation of a hexagonal (CdSe) or zinc blende (ZnSe) crystal lattice (Figure 3). The lack of observable glide-plane defects in single-QD TEM images indicates that the single-source precursor method allows crystalline materials to be readily prepared. The average size and size distribution for the nanocrystals determined from the micrographs correlate well with those predicted from the position and line width of the exciton absorption and photoluminescence bands in Figures 1 and 2. The lack of observable defect emission for nanomaterials larger than 4.0 nm suggests that well-formed II−VI materials can be prepared in HDA.

Because of the air stability of the inorganic clusters, the reactions can be readily scaled to large quantities (1−50 g/L) without substantial adjustment to the growth methodology (Figure 5). Eliminating the pyrolytic event

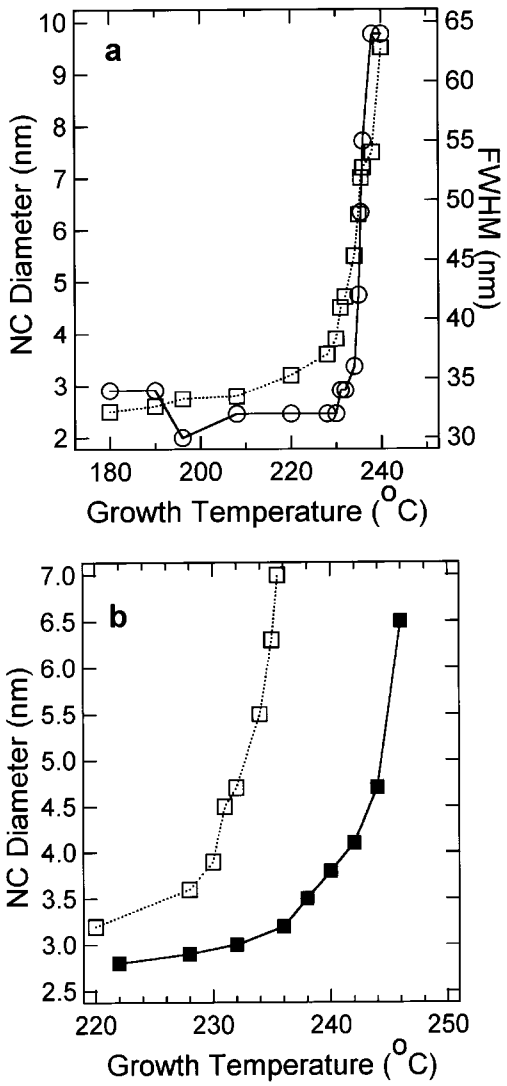

Figure 5. (a) Evolution of the size of the CdSe/HDA nanocrystals (squares) and the fwhm (circles) of the exciton absorbance band with growth temperature. Concentration of the single-source precursor was 6 g/L in HDA. Nanocrystal size was determined from the position of the exciton band. (b) Concentration dependence of the growth rate for CdSe/HDA. Hollow and solid markers represent concentrations of 6 and 17 g/L, respectively, of single-source precursor in HDA.

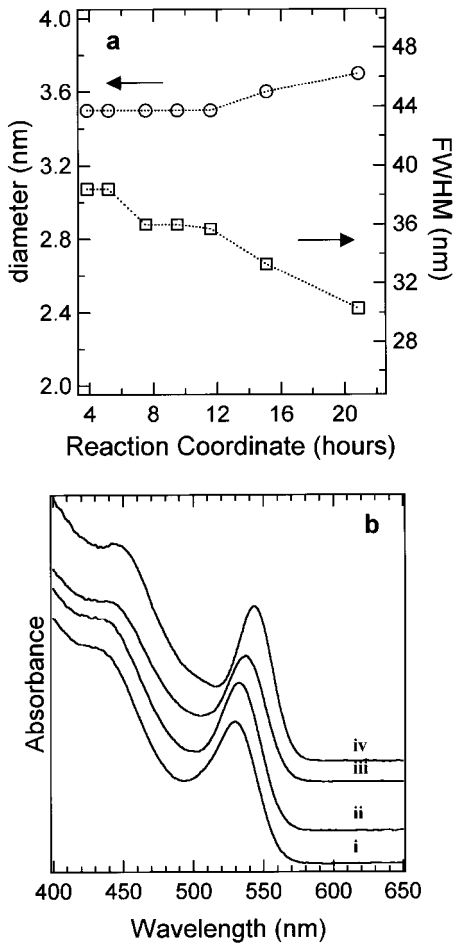

Figure 6. Temporal batch annealing of 3.5-nm CdSe/HDA nanocrystals at 180−190 °C. (a) Change in diameter (circles) and fwhm of the exciton peak (squares) corresponding to a change in distribution from roughly 12% to 5−6%. (b) Change in absorbance spectrum with temporal annealing at (i) 4, (ii) 11.5, (iii) 15, and (iv) 20 h.

for QD formation lowers the temperatures for nanomaterial growth (∼50−75 °C), thus providing greater synthetic control and milder reaction conditions without decreasing material crystallinity. Evidence for nanocrystal growth of CdSe arises from inspection of the absorption data as a function of the growth temperature in Figure 5a. Onset of nanomaterial growth occurs at temperatures in excess of 180 °C. The increase in size of CdSe with increasing reaction temperature illustrates that sustained growth can be achieved in HDA for growth of particles up to 9 nm. Similar results are observed for ZnSe growth conditions except the upper limit for growth is ∼5 nm under the above reaction conditions.

Alkylamines offer a convenient, cheap ligand for nanomaterial passivation, and have been employed for lyothermal preparation of ZnSe.[33a] Because of the weaker interaction strength of the amine in comparison to a phosphine or thiol, the ligand (solvent) is expected to provide the necessary kinetic control to allow for the use of inorganic clusters as a single-source precursor for the growth of nanomaterials. Hexadecylamine was chosen as the growth solvent because of its moderate coordinating capability, high boiling point, and low cost and because of evidence for surface stabilization of the product through chain−chain interactions on the surface, similar to observations in self-assembled monolayers on Au surfaces and Au nanomaterials.[17a,70] We have investigated several alkylamine solvents (6−18 carbons) with similar results; however, lower boiling points tend to lead to smaller nanomaterials or slower growth rates. Growth of materials in trioctyl phosphine also leads to nanomaterials, although the reactions require higher temperature. Reactions in DMF and pyridine do not lead to large materials, possibly because of the lower boiling points of the solvent or stronger coordinating ability of the solvent.

Intriguingly, the nanomaterials exhibit stability in the reaction mixture for extended periods of time (>72 h), allowing for nanomaterial preparation in a batch reactor configuration. At temperatures below 100 °C,

(70) Hostetler, M. J.; Wingate, J. E.; Zhong, C.-J.; Harris, J. E.; Vachet, R. W.; Clark, M. E.; Londono, J. D.; Green, S. J.; Stokes, J. J.; Wignall, G. D.; Glish, G. L.; Porter, M. D.; Evans, N. D.; Murray, R. W. *Langmuir* **1998**, *14*, 17−30.

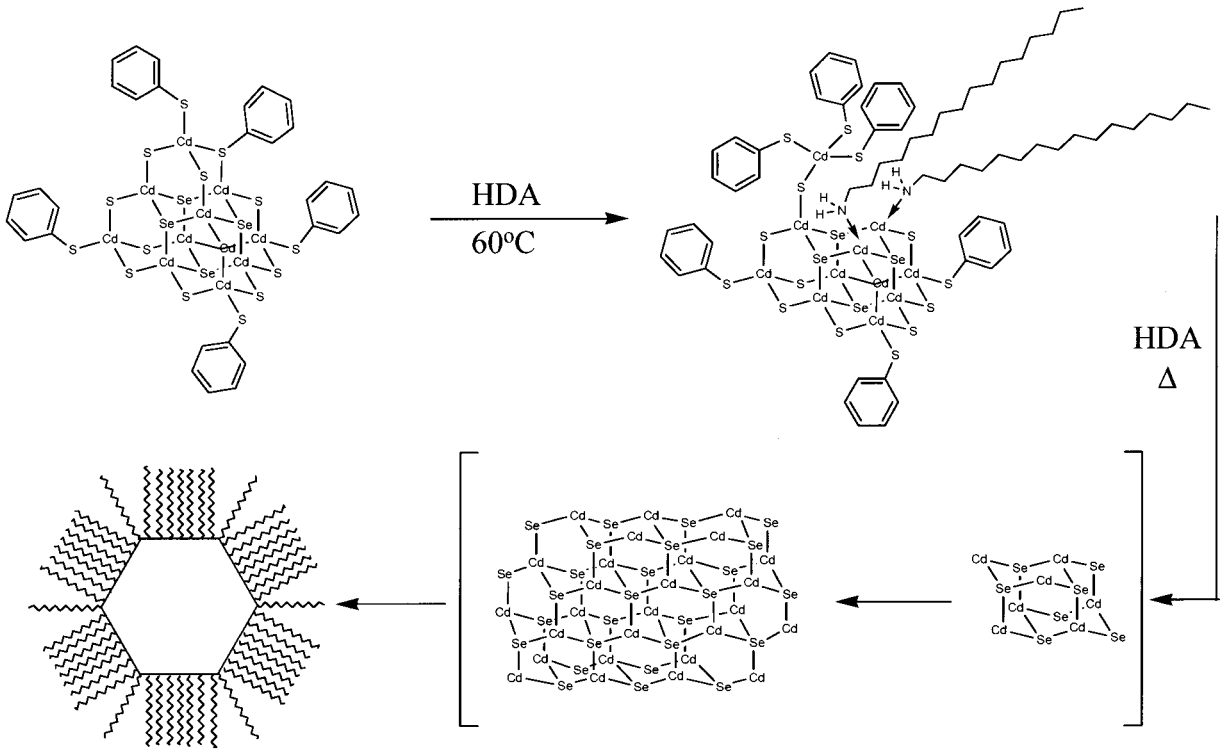

Figure 7. Proposed reaction mechanism for formation of CdSe nanocrystals from cluster precursors. The thiol and amine ligands for the clusters and nanomaterials have been minimized for clarity.

no change or loss of the nanomaterials occurs for extended periods of time in the reaction batch. Storage of the nanocomposites either in hexadecylamine or in octylamine for extended periods under N_2 results in no degradation of either the optical absorption or luminescence properties for periods exceeding 400 h (Supplemental Figure 4). Degradation studies under oxygen indicate that the material quality degrades rapidly, with a broadening of the absorption, a loss of solubility, and a shift to the blue, presumably from oxidation or ligand loss as previously observed in the literature. ZnSe material degradation is extremely rapid, requiring storage under anaerobic conditions.

The as-grown nanomaterials exhibit annealing behavior at the desired size by lowering the growth temperature ~30−40 °C and reacting for 6−12 h to achieve 5% size dispersity out-of-batch (Figure 5). The change in line width from the absorption corresponds to a reduction in line width from 38 to 30 nm fwhm for the exciton (Figure 6) and an improvement in the resolution of the second excitonic transition (Figure 6b, iv). The annealing can be attributed to either changes in the size distribution or improvement in the topology of the nanomaterials due to thermodynamically driven redistribution of the surface atoms. Thermal annealing of the reaction mixture (Figure 6) tightens the distribution to ~5%, allowing ~90% of the material to be collected with tight distributions. Further tightening of the distribution to ≤5% by selected precipitation results in isolation of ~50% of the original quantity in the batch.

The recapping of CdSe nanomaterials with ZnS can be achieved by modification of the standard dimethylzinc organometallic routes.[61] Capping of the nanomaterial surface with an inorganic shell (CdSe/ZnS) gives rise to an increase in the emission QY for CdSe from 6 to 10 to 20%, as has been observed previously, corroborating the formation of the inorganic layer. A close inspection of the XRD data in Supplemental Figure 3 indicates contributions from both the CdSe core and the ZnS overlayer. The absorption data for the core/shell material predict a 3.7-nm CdSe nanomaterial, however, TEM imaging reveals materials of ~5.4 nm, further corroborating the inorganic capping. The low contrast for ZnS makes assignment of the shell thickness based on TEM analysis difficult. This is in accord with previous results on inorganically passivated materials, which exhibit larger crystallite diameters in TEM arising from the shell. Interestingly, the core/shell materials appear triangular in the TEM image, suggesting that lattice strain might influence the nanomaterial morphology via constraints on lattice plane capping.

Mechanism for Growth. The CdSe ratio in CdSe nanomaterials has been reported to be 1.02 based on XPS analysis.[22] The reaction of a $[M_{10}Se_4(SPh)_{16}]^{4-}$ cluster to form a MSe nanomaterial results in a stoichiometry for the reaction of M/Se 2.5:1, significantly higher than expected for the final product. Earlier studies suggest lability of $Cd(SPh)_3^-$, which would still yield a M/Se stoichiometry of 1.5:1 based on the M_6Se_4 core of the cluster. XPS analysis of the CdSe nanomaterials grown in HDA show a ~1:1 ratio of Cd to Se in the final product (Supplemental Figure 5). The lack of stoichiometry in the reaction requires Cd byproducts, which have not been identified. Several possibilities, including Cd amine compounds, Cd thiophenolate, and disulfide species, are expected to be formed and removed during nanomaterial isolation. Excess thiol appears to form disulfide byproducts that pecipitate as a white solid in the reaction mixture. To achieve the proper stoichiometry in the final materials, a thermodynamic nucleus-formation step must initiate the reaction, followed by a

reconstruction of the materials to a thermodynamically favored structure.

Several mechanisms for nucleus formation based on various degrees of cluster fragmentation can be proposed. The mechanism for nucleus formation and growth of nanomaterials must account for the observation of a tight batch distribution, low-temperature nanomaterial growth, and the capacity to reconstruct from a zinc blende core in the clusters to a hexagonal lattice in the CdSe nanomaterial.

One potential mechanism is fragmentation of the M_{10} cluster into M^{2+} and Se^{2-} or poly(metal−chalcogenide) species, followed by reformation of a nucleus, which would give rise to several poorly defined initial nucleus-formation steps. This fragmentation step would be expected to separate nucleus formation poorly from growth, limiting the quality of the final materials. The fragments would be expected to produce larger distributions than observed in the absorption spectra and TEM in Figure 1−3 as a result of uncontrolled growth steps. Attempts to prepare nanomaterials from either $Cd(NO_3)_2$ or $[Cd_4(SPh)_{12}]^{4-}$ and Se in TOP/TOPO, triphenylphosphine selenide, or HDA proceed by an uncontrolled growth mechanism, producing very broad product distributions, thus supporting the lack of complete cluster fragmentation as the initiation step. Broad distributions arising from poor nucleus formation resulting in failure to separate growth have been observed previously in the literature.[23] Intriguingly, the addition of HDA-solubilized Se or Cd in the form of $[M_4(SPh)_{12}]^{4-}$ to growing CdSe nanomaterials has no observable effect on the nanomaterial growth rate, suggesting that Cd−thiophenolate cluster byproducts and complete cluster fragmentation might not make significant contributions to nanomaterial growth.

An alternative mechanism is that the cluster remains intact, acting as partial nuclei, and that nanomaterial growth proceeds by scavenging free M and Se atoms in solution. This mechanism is unsupported by the exchange dynamics of the individual clusters, as observed in previous NMR and ESMS analyses.[48,57,71] The M_{10} systems in a donor solvent such as CH_3CN, DMF, pyridine, or DMSO exhibit rapid ligand and metal ion exchange at the apex of the clusters, which suggests that the clusters will not remain intact upon addition to a nucleophilic solvent.[71] Although the lack of fragmentation would produce well-formed materials, the mechanism is inconsistent with exchange dynamic studies on clusters and cannot account for the structural change from a cubic zinc blende for the Cd_{10} cluster to the hexagonal crystallographic structure for the nanocrystals.

A more likely mechanism for nanomaterial growth can be proposed on the basis of a combination of fragmentation via ring opening and subsequent ligand exchange (Figure 7). A similar mechanism involving facile ring opening, followed by metal or ligand exchange, has been proposed for a series of metal−chalcogenide clusters of various nuclearity based on NMR and ESMS analysis of Cd and Zn clusters in solution in the presence of incoming ligands or metal ions.[48,57,71] In fact, several researchers have proposed that the formation of Cd_{20} and Cd_{32} clusters from Cd_{10} is initiated by ring opening, followed by attack of the exposed Cd atom at the trigonally passivated chalcogenide ion and subsequent loss of the apical $[Cd(SPh)_3]^-$ caps.[51b,51c] In effect, the cluster acts as a template for formation of a larger-nuclearity structure. This mechanism would allow for nucleus formation when the cluster is introduced into the solvent at low temperature, producing a uniform nucleus through ligand exchange. This accounts for the observed nanomaterial monodispersity while allowing structural reorganization to arise from a series of ring-opening events that produce a thermodynamically favored lattice configuration. Although the initial Cd_{10} structure is a cubic zinc blende lattice, the surface energetics of nucleation leads to the formation of a hexagonal lattice for the nanomaterials of CdSe. In ZnSe, the cubic zinc blende lattice of the Zn_{10} precursor is maintained in the final structure.

Conclusion

Molecular clusters of metal−chalcogenide systems, which exhibit facile ligand exchange and structural rearrangements, are analogues of the bulk metal−chalcogenide semiconductor lattice.[53,71] The application of molecular inorganic precursors offers a unique opportunity for growth of nanomaterials at lower temperatures by providing intact nuclei in HDA for the formation of CdSe nanocrystals. The precursor, $(Li)_4[Cd_{10}Se_4(SPh)_{16}]$, can be envisioned as a fragment of the bulk structure that acts as an effective molecular template for growth.[41,42,49] Controlled growth of nanocrystalline II−VI materials is then achieved by thermal control in a moderately coordinating solvent to produce large quantities of nanocrystals that exhibit well-defined crystalline faces, and narrow size/shape dispersion. The use of inorganic clusters in a "seeded-growth" approach results in the inherent versatility of this method. Extension of this methodology allows for the formation of novel binary and ternary semiconductor systems at the nanoscale, which is currently being pursued in our group.

Acknowledgment. This work was supported by the National Science Foundation CAREER Program (DMR9875940).

Supporting Information Available: X-ray powder diffraction data for CdSe, ZnSe, and CdSe/ZnS; absorption spectra illustrating the change in absorption for a CdSe sample in octylamine at room temperature (298 K) for 400 h; and XPS analysis of a 7.0-nm CdSe sample prepared in HDA. This material is available free of charge via the Internet at http://www.pubs.acs.org.

CM010709K

(71) Løver, T.; Henderson, W.; Bowmaker, G.; Seakins, J. M.; Cooney, R. P. *Inorg. Chem.* **1997**, *36*, 3711.